Springer Atmospheric Sciences

Alexander V. Ryzhkov
Dusan S. Zrnic

Radar Polarimetry for Weather Observations

Springer

Springer Atmospheric Sciences

More information about this series at http://www.springer.com/series/10176

Alexander V. Ryzhkov • Dusan S. Zrnic

Radar Polarimetry for Weather Observations

Springer

Alexander V. Ryzhkov
Cooperative Institute for Mesoscale Meteorological Studies
The University of Oklahoma
Norman, OK, USA

Dusan S. Zrnic
National Severe Storms Laboratory
National Oceanic and Atmospheric Administration
Norman, OK, USA

ISSN 2194-5217 ISSN 2194-5225 (electronic)
ISBN 978-3-030-05092-4 ISBN 978-3-030-05093-1 (eBook)
https://doi.org/10.1007/978-3-030-05093-1

Library of Congress Control Number: 2019930082

This Springer imprint is published by the registered company Springer Nature Switzerland AG
The registered company address is: Gewerbestrasse 11, 6330 Cham, Switzerland

Preface

Prior to the advent of dual-polarization radars, direct interpretation of cloud and precipitation bulk characteristics from radar reflectivity was limited to very few unambiguously defined cases, such as the bright band or large hail. Even then, knowledge of the physical conditions, like the height above ground of enhanced reflectivity areas, was needed to properly interpret and quantify the observations. Polarimetry transformed the way meteorologists look at and interpret the bulk properties of clouds and precipitation. It brought a dramatic change to direct interpretation and quantitative assessment of these properties, so much so that the polarimetric weather radar has transitioned from a scientific instrument to operational use. This is exemplified by the network of the US weather surveillance radars (WSR-88D) which have been upgraded to dual-polarization. Several other countries did or are doing similar upgrade of their national weather radar networks. Moreover, some of the weather radar manufacturers do not even offer single-polarization radars for weather surveillance anymore. The additional information dual-polarization radar provides to forecasters is primarily used for quantitative precipitation estimation (QPE), classification of radar returns, discrimination between meteorological and nonmeteorological scatterers, and severe weather warnings. Identification of meteorological scatterers provides an added positive impact on QPE. Potential improvements of QPE were used as principal justifications for the introduction of the Doppler capability (in the 1980s) and dual-polarization upgrade of operational weather radars. Lately, interest is rising within the numerical weather prediction (NWP) community to incorporate polarimetric data into NWP models either via assimilation or through improvement of their microphysical parameterization.

Although there are numerous scientific papers and reports about weather radar polarimetry and its applications, books on the subject are few. We hope that this monograph adds variety and some material not compiled elsewhere. It is meant for practicing radar meteorologists, hydrologists, cloud physicists, and modelers who are interested in the bulk properties of hydrometeors and quantification of these with the goals to improve precipitation measurements, understanding of precipitation processes, or model forecasts. We have made a deliberate attempt to tightly connect

the microphysical processes responsible for the development and evolution of the clouds' bulk physical properties to the polarimetric variables. The book contains instructions on how to simulate realistic polarimetric variables. It also demonstrates that the polarimetric variables from all but the precipitation containing large (Mie) scatterers can be adequately related to bulk precipitation physics using simple closed-form solutions. It also addresses the problem of determining the polarimetric variables from the output of NWP models.

To make the book self-contained, we included fundamental topics in polarimetry such as polarimetric variables, polarimetric radar, and scattering. We hope that the practical aspects, references, and instructions contained herein will be beneficial to those entering this fascinating field as well as to those needing quick answers concerning practical applications of weather radar polarimetry. Much of the material in this book came from the research the authors did at the National Severe Storms Laboratory and the Cooperative Institute for Mesoscale Meteorological Studies. Polarimetric work at the National Severe Storms Laboratory started under the directorship of Dr. E. Kessler and continued under Dr. R. Maddox, Dr. J. Kimpel, and Dr. S. Koch. Crucial were two NSSL radars, first Cimarron and then KOUN, to test various design/engineering aspects of dual polarimetry. These radars also provided valuable data for analysis and interpretation.

The able engineering team responsible for implementation of dual-polarization consisted of D. Sirmans, A. Zahrai, J. Carter, M. Schmidt, and R. Wahkinney. To them and other NSSL support staff, we extend sincere thanks. The National Research Council postdoctoral associates at NSSL, Dr. M. Sachidananda and Dr. N. Balakrishnan, made pioneering contributions at the time when these were most needed. Collaboration with Dr. J. Straka from the University of Oklahoma brought rigor to polarimetric classification of echoes and introduced the subject to the community. Significant contributions to Chaps. 7 and 8 are from Dr. M. Kumjian's works. Discussions with Drs. R. Doviak (NSSL), G. Zhang, V. Melnikov (University of Oklahoma), S. Matrosov (University of Colorado in Boulder), and V. Bringi (Colorado State University) were always illuminating.

We express our deep gratitude to our international partners and colleagues, A. Khain, M. Pinsky, C. Simmer, S. Troemel, K.-E. Kim, D.-I. Lee, G. Lee, R. Kaltenboeck, D. Hudak, S. Boodoo, and many others for their fruitful collaboration and exchange of ideas and data. We also acknowledge help from our colleagues at NSSL/CIMMS, D. Forsyth, T. Schuur, J. Krause, P. Zhang, L. Borowska, H. Reeves, K. Ortega, in the pursuit of our research. The partnership with Drs. R. Palmer and T.-Y. Yu from the Advanced Radar Research Center and their generosity in sharing the OU-PRIME polarimetric data are greatly appreciated.

Last but not least, our students J. Conway, B. Gordon, M. Loney, P, Schlatter, M. Askelson, S. Bachmann, S. Giangrande, S. Ganson, H.-S. Park, J.-Y. Gu, J. Picca, J. Snyder, J. Carlin, P. Bukovcic, D. Mirkovic, E. Griffin, and A. Murphy were sounding boards for testing concepts and ideas, as well as for generating new ones.

Funding for dual-polarization work, although sparse, was sufficient to keep us hungry for more; thank you OAR/NOAA. Token support was provided by the FAA,

NSF, and NASA. Dr. J. Rasmussen, Head of OAR in the 1990s, funded specifically dual-polarization work. Dr. E. Friday, Director of the National Weather Service, arranged the transfer of the WSR-88D (KOUN) from NWS to NSSL. This was a tremendous help to NSSL's research and facilitated the upgrade of the WSR-88D network to dual-polarization.

Norman, OK, USA Alexander V. Ryzhkov
Norman, OK, USA Dusan S. Zrnic

Contents

Abbreviations

α	Canting angle
α	Ratio A/K_{DP}
β	Antenna elevation angle
β	Ratio $A_{\mathrm{DP}}/K_{\mathrm{DP}}$
δ	Backscatter differential phase
ε	Dielectric constant
ε_w	Dielectric constant of water
ε_i	Dielectric constant of solid ice
ε_s	Dielectric constant of snow
η	Reflectivity (cross section per unit volume)
η_o	120π (Ω), free space impedance
θ	Angular distance from the beam axis
θ_e	Elevation angle
θ_1	One-way beamwidth between half-power points
λ	Electromagnetic wavelength
Λ	Slope of the exponential raindrop size distribution
Λ_s	Slope of the exponential size distribution of snow/ice
μ	Shape parameter of the Gamma distribution
ρ_a	Mass density of air
ρ_i	Density of solid ice
ρ_{hv}	Correlation coefficient between horizontally and vertically polarized return signals
$\rho_{xh,xv}$	Correlation coefficients between cross-polar (x) and copolar (h,v) components of the returned signal
ρ_s	Density of snow
ρ_w	Density of water
σ	Width of canting angle distribution
σ_b	Backscattering cross section
σ_e	Extinction or attenuation cross section
σ_v	Doppler spectrum width (m s^{-1})
σ_{vn}	Normalized spectrum width ($4\sigma_{\mathrm{v}}T_s/\lambda$)

σ_θ^2	Second central moment of the two-way antenna radiation pattern
τ	Pulse width
τ_s	Range time delay
ϕ	Azimuth
Φ_{DP}	Differential phase
Ψ	Angle between the axis of rotation of scatterer and the direction of wave propagation
ω	Angular frequency
A_{DP}	Specific differential attenuation (dB km^{-1})
$A_{h,v}$	Specific attenuation at orthogonal polarizations (dB km^{-1})
A_i	Aggregation value for i-th radar echo class
$A_1 - A_5$	Angular moments of particle orientation distributions
c	Speed of light (3×10^8 m s^{-1})
$c_{h,v}$	Speeds of EM waves (polarization H or V) in anisotropic medium
C	Capacitance of particle
CDR	Circular depolarization ratio (dB)
C_{dr}	Circular depolarization ratio (linear units)
D_a	Diameter of the antenna system
D_e	Diameter of an equivalent volume spherical raindrop
D_o	Median volume diameter of particle
D_m	Mean volume (or mass-weighted) diameter of particle
D_v	Diffusivity of water vapor
e	Partial pressure of water vapor
$\mathbf{e}_h$, $\mathbf{e}_v$	Unit vectors in the h and v direction, abbreviated with $\mathbf{e}_{h,v}$
E	Electric field intensity
$\mathrm{E}_{h,v}$	Components of the complex $\vec{\mathbf{E}}$ vector along the $\mathbf{e}_{h,v}$ directions
$E_{h,v}$	Phasor representation of the h and v components
E_w	Saturated vapor pressure with respect to water
E_s	Saturated vapor pressure with respect to ice
$\boldsymbol{E}$	Phasor matrix representation: $\boldsymbol{E} = [E_h, E_v]^T$
$\vec{\mathbf{E}}$	Electric field vector (complex) containing time variation
$\vec{\boldsymbol{E}}$	Phasor vector representation: $\vec{\boldsymbol{E}} = E_h\mathbf{e}_h + E_v\mathbf{e}_v$
f	Frequency
f_d	Doppler frequency shift
f_{rim}	Degree of riming
f_w	Mass water fraction
$f^2(\theta,\phi)$	Normalized one-way power gain of radiation pattern
F	Ventilation coefficient
g	Gravitational constant (9.81 m s^{-2})
g	Antenna gain
$I(\mathbf{r},\mathbf{r}_1)$	Illumination function
$I(t)$	In-phase component of the phasor signal
IWC	Ice water content (g m^{-3})

k	Electromagnetic wave number ($2\pi/\lambda$) in vacuum
K	Thermal conductivity of air
$k_{h,v}$	Complex wave number in atmosphere with scatterers
K_{DP}	Specific differential phase (deg km^{-1})
K_w	$(\varepsilon_w - 1)/(\varepsilon_w + 2)$
K_i	$(\varepsilon_i - 1)/(\varepsilon_i + 2)$
$l_{h,v}$	One-way propagation loss due to scatter and absorption (≥ 1)
ln	Natural logarithm
log	Logarithm to base 10
$\boldsymbol{L}$	Matrix of losses
$L_{a,b}$	Shape factors of spheroidal particle
$l_{h,v}$	Loss factors at orthogonal polarizations (≥ 1)
l_r	Range weighting function loss factor (≥ 1)
L_f	Latent heat of fusion (melting)
L_r	10 log l_{r} (dB)
L_v	Latent heat of vaporization
LDR	Linear depolarization ratio (dB)
L_{dr}	Linear depolarization ratio (linear units)
LWC	Liquid water content (g m^{-3})
m	Mass of particle
M	Number of signal samples (or sample pairs) along sample time axis
M_{I}	Number of independent samples
$n_{h,v}$	Refractive index (complex) of atmosphere with hydrometeors
$\Delta n^{(\mathrm{air})}$	Contribution to refractive index by air
$\Delta n_{h,v}^{(\mathrm{scat})}$	Contribution to refractive index by scatterers (hydrometeors)
$N_{h,v}$	White noise power in the orthogonal receiver channels
$N(D_e)$	Drop size distribution (m^{-3} mm^{-1})
N_{Re}	Reynolds number
N_0	Intercept parameter of the exponential and gamma size distribution of raindrops
N_{0s}	Intercept parameter of the exponential size distribution of ice/snow
N_w	Intercept parameter of the normalized size distribution of raindrops
$N_0{}^*$	Intercept parameter of the normalized size distribution of ice/snow
N_t	Total concentration of particles (m^{-3})
P	Atmospheric pressure
P^r	Received signal power
P^t	Peak transmitted power
$P^{(i)}(V_j)$	Membership function of the variable "j" and class "i"
PIA	Two-way path-integrated attenuation (dB)
PIA	Two-way path-integrated attenuation in linear scale
Q_w	Total water content
$Q(t)$	Quadrature-phase component of the complex signal
r	Range to scatterer
r_a	Unambiguous range

r_6	6-dB range width of resolution volume
$\mathbf{r_o}$	Vector range to the resolution volume V_6 center
r_m	Aspect ratio of melting graupel/hail
r_w	Axis ratio of raindrops
R	Rain rate (mm h^{-1})
RH	Relative humidity of air (%)
$R_{hh,vv}(T_s)$	Autocorrelations of weather signal
R_{hv}	Cross-correlation of weather signals of H and V polarization
R_v	Gas constant for water vapor
$s^{(0)}_{hh,vv}$	Forward-scattering coefficient of a scatterer
s_{mn}	Backscattering coefficient of a scatterer, incident polarization is n (H or V), backscattered is m (H or V)
$s_{a,b}$	Backscattering coefficients of a spheroidal scatterer: subscript a is for incident polarization parallel to the rotation axis and subscript b for incident polarization perpendicular to this axis
$\vec{\mathbf{S}}$	Power density of the electromagnetic wave
$\mathbf{S}$	Scattering matrix
S	Snow water equivalent rate (mm h^{-1})
S_w	Vapor saturation ratio with respect to water
S_i	Vapor saturation ratio with respect to ice
SNR	Signal-to-noise ratio (dB)
snr	Signal-to-noise ratio (linear scale)
$\mathbf{T}$	Transmission matrix
T_s	Pulse repetition time
T	Temperature in C^o
v	Doppler velocity (m s^{-1})
V_6	Resolution volume size
$V_{hh,vv}$	Voltage complex representations (contains $j2\pi f$)
$V_{hh,vv}$	Voltage phasor representations
V_t	Terminal velocity of hydrometeor (m s^{-1})
$W(r)$	Range weighting function
$Z_{H,V}$	Reflectivity factors for horizontal and vertical polarizations (dBZ)
$Z_{h,v}$	Reflectivity factors for horizontal and vertical polarizations (mm^6 m^{-3})
Z_{dr}	Differential reflectivity in linear units (Z_h/Z_v)
Z_{DR}	Differential reflectivity (dB)
Z_{DP}	Reflectivity difference ($Z_h - Z_v$) in mm^6 m^{-3}

Chapter 1
Polarization, Scattering, and Propagation of Electromagnetic Waves

Understanding polarimetric measurements requires basic knowledge of interaction between electromagnetic (EM) waves and hydrometeors like raindrops, snowflakes, hailstones, or graupel. These particles extract energy from the EM waves and scatter it in all directions and hence are named scatterers. Some, like raindrops, are preferentially oriented and, therefore, interact differently with EM fields than more randomly oriented scatterers like snow aggregates. The number of scatterers interacting with propagating wave is very large and so is the number reflecting the wave. The impact of propagation and reflection on the wave is quantified by the weather radar. Radar measurements are examined with the aim to characterize the bulk properties of the involved scatterers (average concentration, size, shape, orientation, and phase composition). From the bulk properties, the type of hydrometeors in the cloud can be inferred and the amount of precipitation estimated. Telling by remote means the type and amount of precipitation on the ground has been a long-standing goal of meteorologists. The polarimetric radar has promise of achieving this goal.

Fundamental to the scatterers' bulk properties are the scattering characteristics of a single hydrometeor. These are introduced here and quantified in terms of scatterer's physical properties. The concept is then applied to determine propagation effects through the atmosphere filled with a collection of hydrometeors. These effects manifest themselves as attenuation and phase shift of the EM wave. Useful formulas are derived anticipating applications for measurements of bulk precipitation properties.

1.1 Polarization State of Electromagnetic Wave

Coupled fields of electric and magnetic force propagating in space are called electromagnetic (EM) waves. A packet of these waves has spatial and temporal variation of the electric and magnetic fields. Most fields generated by humans for

A. V. Ryzhkov, D. S. Zrnic, *Radar Polarimetry for Weather Observations*,
Springer Atmospheric Sciences, https://doi.org/10.1007/978-3-030-05093-1_1

transmitting information (communication, entertainment, etc.) and remote sensing with radar have sinusoidal variations. Natural sources of EM propagating fields emanating from stars, sun, or lightning discharge do not have simple sinusoidal variations.

At far distance from a source, the vectors of electric and magnetic fields lie in a plane perpendicular to the propagation direction **k** and are perpendicular to each other. This plane is called polarization plane and is defined with two orthogonal directions **h** (horizontal) and **v** (vertical). It is convenient and physically meaningful to designate the horizontal direction as parallel to the locally flat earth surface. Polarization refers to the orientation of the electric field in the polarization plane. The electric field vector of a plane electromagnetic wave traveling in the **r** direction can be expressed in complex notation as a sum of horizontally and vertically polarized components $\vec{\mathbf{E}}_h$ and $\vec{\mathbf{E}}_v$ (Fig. 1.1)

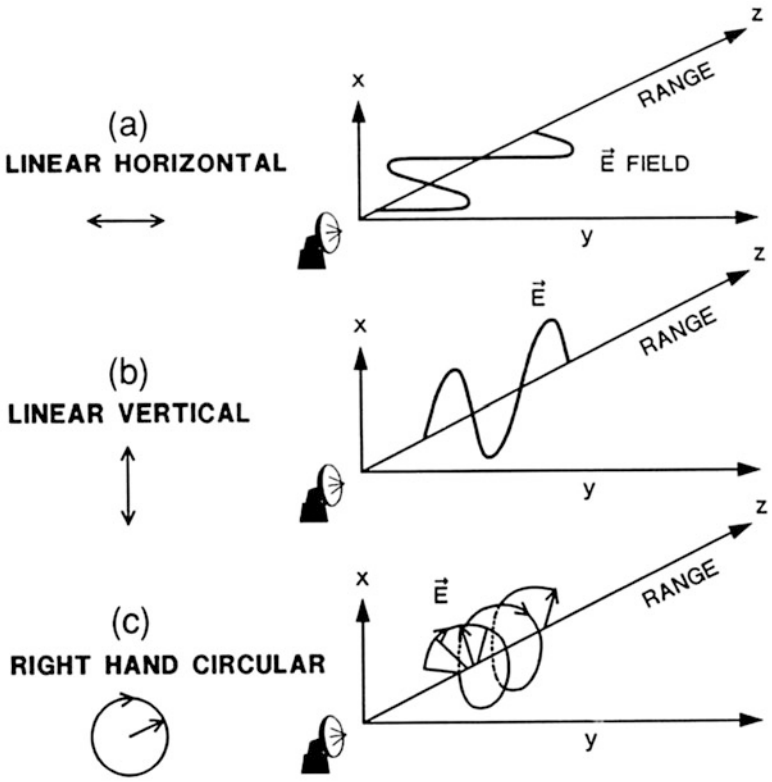

Fig. 1.1 The spatial dependence of the electric field vector for (**a**) horizontally, (**b**) vertically, and (**c**) circularly (right-handed) polarized waves. From Doviak and Zrnic (2006)

$$\vec{\mathbf{E}}(r) = \underset{h}{\vec{\mathbf{E}}}(r) + \underset{v}{\vec{\mathbf{E}}}(r) = \mid E_h(0) \mid \exp[j(2\pi ft - k_h r - \varphi_h)]\mathbf{e}_h + \mid E_v(0) \mid \exp[j(2\pi ft - k_v r - \varphi_v)]\mathbf{e}_v, \left(\mathrm{V\,m^{-1}}\right) \tag{1.1}$$

where $\mathbf{e}_h$ and $\mathbf{e}_v$ are the unit vectors corresponding to the horizontal and vertical polarizations, $|E_h(0)|$ and $|E_v(0)|$ are the amplitudes of horizontally and vertically polarized components of the electric field at $r = 0$, $t = 0$, t is time (s), f is frequency (Hz), $\varphi_{h,v}$ are initial phases (i.e., $E_{h,v}(0) = |E_{h,v}(0)|\exp(-j\varphi_{h,v})$), and $k_{h,v}$ are wave numbers defined as

$$k_{h,v} = 2\pi n_{h,v} f/c \left(\mathrm{m^{-1}}\right). \tag{1.2}$$

In (1.2), c is the speed of light in vacuum and n_h and n_v are the refractive indices of the propagation medium with respect to horizontal and vertical polarizations. In the atmosphere, the refractive indices are complex numbers; the real parts quantify phase shift in (1.1) and imaginary parts quantify attenuation. In vacuum, $n_{h,v} = 1$ and

$$k_{h,v} = k = 2\pi f/c = 2\pi/\lambda \left(\mathrm{m^{-1}}\right), \tag{1.3}$$

where λ is the wavelength. It is understood that the actual fields are real parts of Eq. (1.1) obtained by replacing the exponents with cosines of the arguments (without the imaginary unit j).

In a homogeneous medium having refractive indexes $n_{h,v}$, the EM wave propagates at the speed

$$c_{h,v} = c/\mathrm{Re}(n_{h,v}) \left(\mathrm{m\,s^{-1}}\right). \tag{1.4}$$

The refractive indices are related to the dielectric constants of the medium at orthogonal polarizations ε_h and ε_v as $n_{h,v} = \sqrt{\varepsilon_{h,v}}$. The purposeful distinction between refractive index for horizontally and vertically polarized waves is to quantify propagation of both in the atmosphere filled with nonspherical oriented hydrometeors. At microwave frequencies, the pair of refractive index values $n_{h,v}$ is

$$n_{h,v} = 1 + \Delta n^{(\mathrm{air})} + \Delta n_{h,v}^{(\mathrm{scat})}. \tag{1.5}$$

In (1.5), the component $\Delta n^{(\mathrm{air})}$ represents the contribution of atmospheric gases causing refraction or bending of the wave propagation path (Doviak and Zrnic 2006) and attenuation of the propagating EM field (Ulaby et al. 1981). The real part of the refractive index due to atmospheric gases is

$$\mathrm{Re}\left(\Delta n^{(\mathrm{air})}\right) = \frac{77.6}{T}\left(P + \frac{4810e}{T}\right)10^{-6}, \tag{1.6}$$

where P is the atmospheric pressure (in millibars), e is the partial pressure of water vapor (in millibars), and T is the temperature (in °K). The imaginary part of $\Delta n^{(\mathrm{air})}$ quantifies gaseous absorption. The term $\Delta n_{h,v}{}^{(\mathrm{scat})}$ in (1.5) describes the contribution of atmospheric scatterers (hydrometeors, biota, and others). The contributions at the horizontal and vertical polarizations (H, V) differ if the scatterers are nonspherical and oriented. Hydrometeors such as raindrops or ice crystals falling under the influence of gravity are oriented by drag forces; therefore, generally $\Delta n_h{}^{(\mathrm{scat})} \neq \Delta n_v{}^{(\mathrm{scat})}$.

To explicitly express the wave dependence on attenuation and phase shift represented by the terms $[\mathrm{Im}(k_{h,v})r]$ and $[\mathrm{Re}(k_{h,v})r]$, Eq. (1.1) is rewritten as

$$\mathrm{Re}\left[\vec{\mathbf{E}}\,(r)\right] = \mid E_h(r) \mid \cos\left(2\pi ft - \mathrm{Re}(k_h)r - \varphi_h\right)\mathbf{e}_h + \mid E_v(r) \mid \cos\left(2\pi ft - \mathrm{Re}(k_v)r - \varphi_v\right)\mathbf{e}_v, \tag{1.7}$$

where

$$\mid \mathrm{E}_{h,v}(r) \mid = \mid \mathrm{E}_{h,v}(0) \mid \exp[\mathrm{Im}(k_{h,v})r], \quad \mathrm{Im}(k_{h,v}) < 0. \tag{1.8}$$

Equation (1.7) quantifies how the real part of the wave number (or refractive index) affects the phase of the propagating wave. Through (1.8), the imaginary part quantifies attenuation by the medium filled with atmospheric gases and hydrometeors.

At any given range r, the vectors of horizontally and vertically polarized components of the wave oscillate with frequency f along directions defined by the unit vectors $\mathbf{e}_h$ and $\mathbf{e}_v$. The direction of the composite vector $\mathrm{Re}\left[\vec{\mathbf{E}}\,(r)\right]$ depends on the phase difference, $\Delta\varphi$, between the orthogonal components of the wave:

$$\Delta\varphi = \mathrm{Re}(k_h - k_v)r + \varphi_h - \varphi_v. \tag{1.9}$$

If $\Delta\varphi$ is an integer multiple of π, then the horizontally and vertically polarized components of the electric field are in phase or out of phase and the vector $\mathrm{Re}\left(\vec{\mathbf{E}}\right)$ oscillates along a fixed line, i.e., the electromagnetic wave is linearly polarized (Fig. 1.2a). Otherwise, the instantaneous direction of the vector $\mathrm{Re}\left(\vec{\mathbf{E}}\right)$ changes in time and its tip describes an ellipse; hence, that polarization state is called elliptical (Fig. 1.2b).

If $|E_h(r)| = |E_v(r)|$ and $\Delta\varphi = \pm\pi/2$, the ellipse becomes a circle and the polarization is circular. The electric vector $\mathrm{Re}\left(\vec{\mathbf{E}}\right)$ rotates in the clockwise direction (when viewed in the direction of propagation) if $\Delta\varphi = \pi/2$ (Fig. 1.2c) and in the counterclockwise direction if $\Delta\varphi = -\pi/2$ (Fig. 1.2d). The corresponding polarization states are, respectively, called right-hand circular and left-hand circular. This convention of viewing the vector in the direction of propagation is adopted here. Viewing reflected waves from the propagation direction is standard in the optical community and a

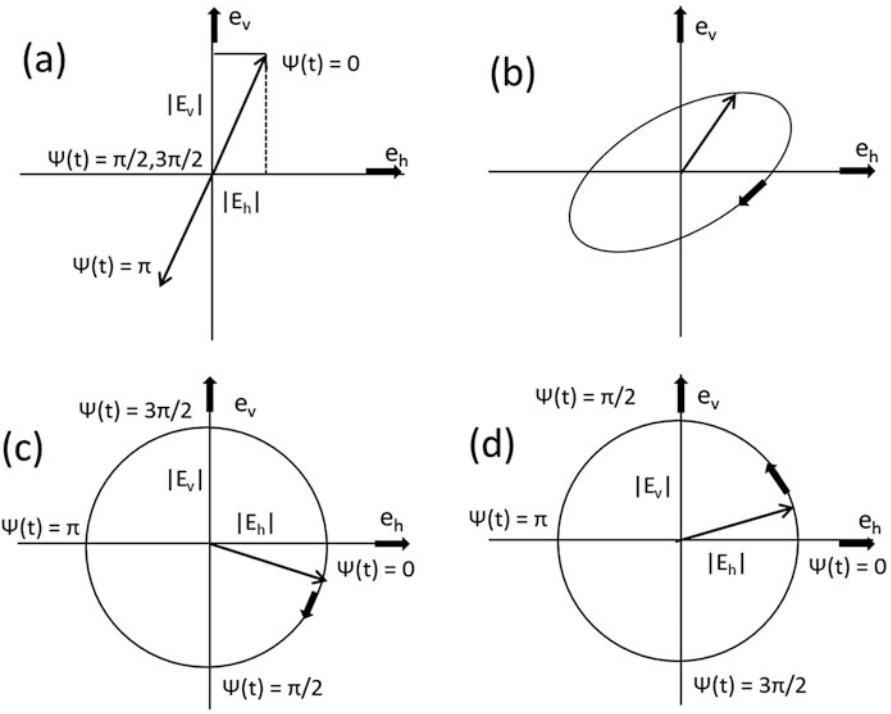

Fig. 1.2 Vector of electric field and trajectories of its tip for (**a**) linear polarization, (**b**) elliptical polarization, (**c**) right-hand circular polarization, and (**d**) left-hand circular polarizations; $\psi(t) = 2\pi ft - \Delta\varphi$ (see (1.7) and (1.9))

comprehensive discussion of the two conventions is in the book by Bringi and Chandrasekar (2001). Note the phase difference (1.9) depends on r if $k_h \neq k_v$. Therefore, the polarization state of the wave changes as it propagates in an anisotropic medium.

It is a standard practice to separate the time-varying factor $\exp(j2\pi ft)$ in the expression (1.1) for complex electric vector

$$\vec{\mathbf{E}}\,(r) = E_h \exp(j2\pi ft)\mathbf{e}_h + E_v \exp(j2\pi ft)\mathbf{e}_v \left(\mathrm{V\,m^{-1}}\right) \tag{1.10}$$

and analyze the pair of complex amplitudes $E_{h,v}$ referred to as phasors. In matrix notation, the phasor pair is expressed as

$$\boldsymbol{E} = \begin{bmatrix} E_h \\ E_v \end{bmatrix} = \begin{bmatrix} E_h(0)\exp(-jk_h r - j\varphi_h) \\ E_v(0)\exp(-jk_v r - j\varphi_v) \end{bmatrix} \left(\mathrm{V\,m^{-1}}\right). \tag{1.11}$$

In the sequel concerning (1.11) and similar equations, capital italics denote the phasors, capital letters indicate complex quantities containing the time-varying

factor $\exp(j2\pi ft)$, and unit vectors (i.e., $\mathbf{e}_h$ or $\mathbf{e}_v$) are explicitly added to clarify the physical meaning behind some derivations.

A propagating wave carries power in the direction of propagation, and the *instantaneous* power density $\left|\vec{\mathbf{S}}\right|$ is the magnitude of the vector product of electric and magnetic fields (Popovic 1971):

$$\left|\vec{\mathbf{S}}\right| = \left|\vec{\mathbf{E}} \times \vec{\mathbf{H}}\right| = \left|\vec{\mathbf{E}}\right|^2 / \eta_0 \left(\mathrm{W\,m^{-2}}\right). \tag{1.12}$$

This definition is valid for plane waves propagating in free space where $\eta_0 = 377\ \Omega$ (ohm) is the free space impedance; it relates the electric and magnetic fields via $\left|\vec{\mathbf{H}}\right| = |\vec{\mathbf{E}}| / \eta_0$. At a given range r, the instantaneous power density varies rapidly between zero and its maximum. It is the average power density $\overline{|\vec{\mathbf{S}}|}$ over one cycle $T_c = 1/f$ of the wave that matters and can be quantified by standard measuring instruments. In vacuum,

$$\begin{aligned} \overline{|\vec{\mathbf{S}}|} &= \frac{1}{\eta_0 T_c} \int_0^{T_c} |\mathrm{Re}(\mathbf{E})|^2 dt \\ &= \frac{1}{\eta_0 T_c} \int_0^{T_c} \left[E_h^2 \cos^2(2\pi ft - kr - \varphi_h) + E_v^2 \cos^2(2\pi ft - kr - \varphi_v)\right] dt \end{aligned} \tag{1.13}$$

and simplifies to

$$\overline{|\vec{\mathbf{S}}|} = \frac{E_h^2 + E_v^2}{2\eta_0} = \frac{|\boldsymbol{E}|^2}{2\eta_0} \left(\mathrm{W\,m^{-2}}\right). \tag{1.14}$$

It is evident in (1.14) and intuitively satisfying that the circularly polarized wave (i.e., $E_h = E_v$ and phase difference 90°) carries twice the power of its constituent horizontal and vertical projections.

1.2 Scattering by a Single Particle

Next we consider a plane wave impinging on a scatterer. The wave induces oscillating currents within the scatterer. These currents may not be collinear with the incident electric field direction and produce secondary radiation in all directions including opposite to the incident wave. Although the following exposition concerns a continuous wave, it is applicable to pulsed sinusoidal waves typically emitted by

weather surveillance radars; thereby the leading edge of the wave causes transients in the scattered field. These transients decay very fast (in few cycles) compared to the duration of the pulse (hundreds of cycles). Therefore, the steady state is quickly established and its temporal variation expressed by $\exp(j2\pi ft)$ is implicitly assumed throughout the book.

The strength of electric field produced by the scatterer is inversely proportional to the distance r as can be deduced from the following physical considerations. Assume the scatterer intercepts electromagnetic wave with a power density expressed by (1.14). Some of the intercepted energy is reradiated back toward the radar, some in other directions, and some is absorbed and dissipated inside the scatterer. The total power of the scattered radiation (in a lossless medium) passing through a sphere centered on the scatterer doesn't depend on the sphere radius r; hence the power density is inversely proportional to r^2. Therefore, the electric field corresponding to the scattered radiation is inversely proportional to r. Relevant to radar measurements is the portion radiating back and its relation to the backscatter cross section of a scatterer (Doviak and Zrnic 2006, Sect. 3.2).

For quantifying effects of propagation and reflections from an ensemble of hydrometeors, consideration of scattering in several directions is needed. Hence we next present the matrix form of the scattering equation but assume propagation in vacuum. The derived results are valid for other isotropic and nonattenuating media (only the wave number must be modified). Extension to anisotropic media (e.g., precipitation) is made in Chap. 2. With this simplification, we isolate the scatterer's properties from propagation effects (quantified in Sect. 1.3).

The scattering matrix $\mathbf{S}$ relates two orthogonal components of the scattered field $\boldsymbol{E}^s$ to the orthogonal components of the incident field $\boldsymbol{E}^i$ and it is defined by (e.g., Bohren and Huffman 1983)

$$\boldsymbol{E}^{\mathrm{s}} = \frac{e^{-jkr}}{r}\mathbf{S}\boldsymbol{E}^i \left(\mathrm{V\,m^{-1}}\right), \tag{1.15}$$

where r is the distance between the particle and the measurement location of $\boldsymbol{E}^s$ (very far from the scatterer), and the intervening attenuation is negligible (propagation medium is vacuum). Equation (1.15) in expanded form is written as

$$\begin{bmatrix} E_h^s \\ E_v^s \end{bmatrix} = \frac{e^{-jkr}}{r} \begin{bmatrix} s_{\mathrm{hh}}(\mathbf{k}_i, \mathbf{k}_s) & s_{\mathrm{hv}}(\mathbf{k}_i, \mathbf{k}_s) \\ s_{\mathrm{vh}}(\mathbf{k}_i, \mathbf{k}_s) & s_{\mathrm{vv}}(\mathbf{k}_i, \mathbf{k}_s) \end{bmatrix} \begin{bmatrix} E_h^i \\ E_v^i \end{bmatrix}, \tag{1.16}$$

to explicitly identify the complex amplitudes (phasors) $E_h^{i,s}$ and $E_v^{i,s}$ of horizontally and vertically polarized components of the incident and scattered fields in the coordinate system associated with the unit vector $\mathbf{k}_i$ corresponding to the direction of the propagating incident wave (Fig. 1.3).

If $\mathbf{k}_s = \mathbf{k}_i$ the matrix $\mathbf{S}$ is called the forward-scattering matrix ($\mathbf{S}^{(0)}$), and it is called the backscattering matrix ($\mathbf{S}^{(\pi)}$) if $\mathbf{k}_s = -\mathbf{k}_i$. The superscript indicates the angle between vectors $\mathbf{k}_s$ and $\mathbf{k}_i$. Generally $\mathbf{S}^{(0)} \neq \mathbf{S}^{(\pi)}$. For radar measurements, the

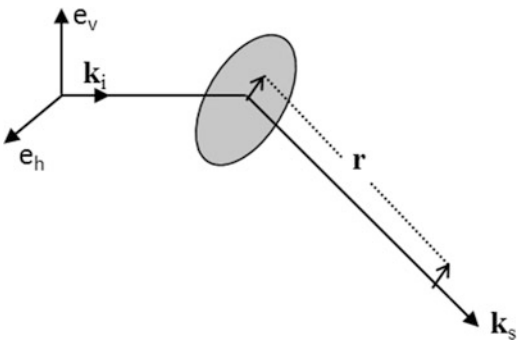

Fig. 1.3 Scattering geometry including coordinate systems and propagation vectors. Superscript *i* indicates incident field and *s* stands for scattered field

backscattering matrix is of primary interest because it relates the properties of the transmitted radiation and backscattered radiation (carrying information about hydrometeors) at the radar location. Henceforth the superscript will be dropped from the backscattering matrix, so that

$$\mathbf{S}=\begin{bmatrix} s_{\mathrm{hh}} & s_{\mathrm{hv}} \\ s_{\mathrm{vh}} & s_{\mathrm{vv}} \end{bmatrix} (\mathrm{m}), \tag{1.17}$$

and, for short, it will be called the scattering matrix.

The term s_{mn} is called backscattering (or backscatter) coefficient. Its second subscript (n) indicates the polarization (h or v) of the incident field transmitted by the radar; its first subscript refers to the polarization of the backscattered field. The coefficient represents intrinsic (inherent) electromagnetic properties of the scatterer causing the radar return. It is complex and its magnitude quantifies the portion of the incident field reflected back whereas its phase indicates the shift upon reflection (backscattering) with respect to the phase of the incident field. Determining the value of s_{mn} for various scatterers can be quite complicated and is a discipline in itself. Nonetheless, certain types of scatterers (spheroids) at wavelengths large compared to scatterers' dimensions offer closed-form solutions (Chap. 5).

The matrix description of scattering is needed because many scatterers in the atmosphere change polarization of the incident EM radiation. Therefore the scattered field $\boldsymbol{E}^s$ contains two orthogonal components (horizontally and vertically polarized) even if the incident wave $\boldsymbol{E}^i$ contains only one. The off-diagonal elements of the scattering matrix $\mathbf{S}$ are equal, i.e., $s_{\mathrm{hv}} = s_{\mathrm{vh}}$. The equality stems from reciprocity principle applicable to passive media. For our purpose, the principle can be phrased as follows. If horizontally polarized field illuminates a scatterer and vertically polarized reflected field is measured, the result is the same as would be obtained if vertically polarized fields were illuminating the scatterer and horizontally polarized fields were measured. Throughout the book, s_{hv} always equals s_{vh}, but for proper association with the transmitted and received polarization, both symbols are often used.

Computations of the elements of the scattering matrix for hydrometeors of complex shapes are generally complicated (particularly for scatterers comparable or larger than the wavelength) and require evaluation of the distributions of the fields inside the scatterer. This, even for ellipsoids, is not trivial. Significant simplification occurs if scatterers are spheroids. These shapes accurately approximate raindrops and graupel and are quite adequate for snowflakes, ice crystals, small hailstones, or insects. In this book, spheroids are considered for modeling scatter of most hydrometeors.

Scattering properties of a spheroid can be represented by a combination of two crossed dipoles oriented along the axis a and b of the projected spheroid onto the plane of polarization. The angle between the projection of the rotation axis a on the plane of polarization and the direction of the vertical electric field is called the canting angle and will be denoted with α. The dipole model is applicable to small arbitrarily shaped hydrometeors and the spheroid approximation (oblate or prolate) is used to model the flat or elongated ones.

If the direction of the incident electric field $\underset{i}{\vec{\mathbf{E}}}$ coincides with the direction of one of the dipoles, then only that particular dipole is excited to produce secondary radiation in the same "copolar" direction as the incident field. This happens, for example, if a raindrop is illuminated by horizontally polarized waves. Raindrops have approximately oblate shapes and their rotation axis a is vertically oriented (see Chap. 4). In this case, polarization of the backscattered wave is also horizontal (Fig. 1.4a). For this specific geometry, the backscatter coefficient $s_{\mathrm{hh}} = s_b$ is called the backscattering amplitude along the axis b, and in the absence of attenuation, the relation (1.15) between backscattered (indicated with superscript b) and incident field (phasor representation) becomes

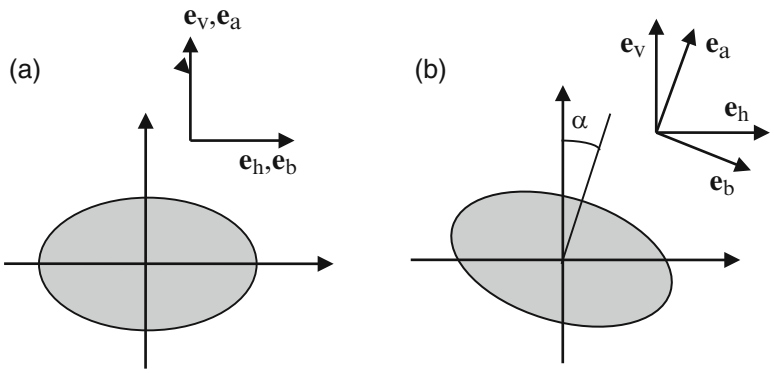

Fig. 1.4 Cross sections in the plane of polarization of (**a**) noncanted and (**b**) canted hydrometeor. Non-depolarizing orientation is on the left and the depolarizing one is on the right

$$E_h^b \mathbf{e}_h = \frac{e^{-jkr}}{r} s_b E_h^i \mathbf{e}_h. \tag{1.18}$$

The same raindrop will produce vertically polarized backscattered wave if the polarization of incident wave is vertical, thus

$$E_v^b \mathbf{e}_v = \frac{e^{-jkr}}{r} s_a E_v^i \mathbf{e}_v, \tag{1.19}$$

where $s_a = s_{vv}$ is the backscattering amplitude along the vertical (rotation) axis a.

If the raindrop is canted in the plane of polarization, then the principal axes of the canted raindrop are not vertical or horizontal (Fig. 1.4b). Both dipoles are excited and each generates secondary radiation along its axis. The vector of horizontally polarized incident field can be represented as a sum of two components aligned with the two principle axes a and b

$$E_h^i \mathbf{e}_h = E_h^i \cos\alpha \mathbf{e}_b + E_h^i \sin\alpha \mathbf{e}_a = E_b^i \mathbf{e}_b + E_a^i \mathbf{e}_a, \tag{1.20}$$

where $\mathbf{e}_a$ and $\mathbf{e}_b$ are the unit vectors directed along a and b axes. These unit vectors are related to the unit vectors $\mathbf{e}_h$ and $\mathbf{e}_v$ via the rotation transformation as

$$\begin{bmatrix} \mathbf{e}_a \\ \mathbf{e}_b \end{bmatrix} = \begin{bmatrix} \sin\alpha & \cos\alpha \\ \cos\alpha & -\sin\alpha \end{bmatrix} \begin{bmatrix} \mathbf{e}_h \\ \mathbf{e}_v \end{bmatrix}. \tag{1.21}$$

The backscatter fields from the two diploes are proportional to the product of the incident field components (E_a^i and E_b^i) along their axes and backscattering amplitudes s_a and s_b. Consider a horizontally polarized incident field with magnitude E_h^i. Then

$$\begin{aligned} \vec{\boldsymbol{E}}^b &= \frac{e^{-jkr}}{r}\left(s_a E_a^i \mathbf{e}_a + s_b E_b^i \mathbf{e}_b\right) \\ &= \frac{e^{-jkr}}{r}\left[E_h^i\left(s_a \sin^2\alpha + s_b \cos^2\alpha\right)\mathbf{e}_h + E_h^i (s_a - s_b)\sin\alpha\cos\alpha \mathbf{e}_v\right], \end{aligned} \tag{1.22}$$

and the backscattered field $\vec{\boldsymbol{E}}^b$ has both horizontal and vertical components if $s_a \neq s_b$. For vertically polarized incident field, similar derivation yields

$$\vec{\boldsymbol{E}}^b = \frac{e^{-jkr}}{r}\left[E_v^i (s_a - s_b)\sin\alpha\cos\alpha \ \ \mathbf{e}_h + E_v^i\left(s_b \sin^2\alpha + s_a \cos^2\alpha\right)\mathbf{e}_v\right]. \tag{1.23}$$

Compacting (1.22) and (1.23) into a matrix equation produces the following expression for the backscattering matrix of a single spheroidal particle whose axis of rotation is in the plane of polarization:

$$\mathbf{S} = \begin{bmatrix} s_a \sin^2\alpha + s_b \cos^2\alpha & (s_a - s_b)\sin\alpha\cos\alpha \\ (s_a - s_b)\sin\alpha\cos\alpha & s_b \sin^2\alpha + s_a \cos^2\alpha \end{bmatrix} (\mathrm{m}). \tag{1.24}$$

The expression (1.24) applies to a spheroid whose axis of rotation lies in the plane of polarization of the incident wave, therefore the angle ψ between the axis of rotation and the direction of wave propagation is $\pi/2$. If $\psi \neq \pi/2$ (Fig. 1.5), the backscattering amplitudes s_a and s_b in (1.19) should be replaced with the amplitudes s'_{hh} and s'_{vv} that are functions of the angle ψ (Holt 1984). It was shown by Holt and Shepherd (1979) that such dependencies on ψ are simple if scatterers are much smaller than the wavelength. Then the following "backscatter rule" applies

$$s'_{\mathrm{hh}} = s_b \ (\mathrm{m}) \tag{1.25}$$

$$s'_{\mathrm{vv}} = s_a \sin^2\psi + s_b \cos^2\psi \, (\mathrm{m}). \tag{1.26}$$

To grasp the physical meaning behind (1.26), assume that there is no canting in the polarization plane ($\alpha = 0$), the direction of wave propagation **k** is in the horizontal plane ($\beta = 0$), and the symmetry axis of oblate spheroid **N** rotates from $\psi = \pi/2$ to $\psi = 0$ in the vertical plane x–z (Fig. 1.5). Then the projection of the spheroid onto the polarization plane x–y varies as shown in Fig. 1.6. It is obvious that the horizontal dimension of the projection (b) (proportional to the radar return at horizontal polarization) remains the same, while its vertical projection increases from a (at $\psi = \pi/2$) to b (at $\psi = 0$). In other words, s_{hh} remains equal to s_b, whereas s_{vv} changes from s_a to s_b as reflected in Eq. (1.26).

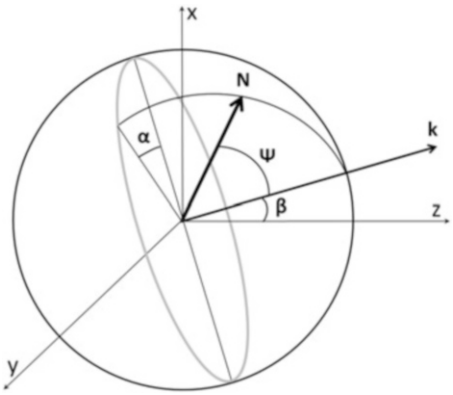

Fig. 1.5 Scattering geometry. Direction **N** denotes orientation of the symmetry axis of the particle, **k** represents the direction of wave propagation; it is perpendicular to the polarization plane and lies in the x, z plane. The polarization plane is depicted by the grey ellipse. The x axis is true vertical and y z is horizontal direction. Canting angle α is the angle between the projections of vector **N** and true vertical x on the polarization plane, ψ is the angle between **N** and **k**, and antenna elevation angle is β

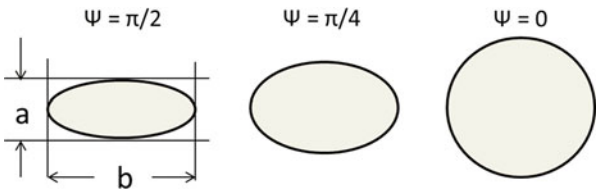

Fig. 1.6 Spheroid projection onto the polarization plane for different values of ψ

Holt and Shepherd (1979) indicate that the backscatter rule applies for oblate raindrops up to 35 GHz provided $\psi > 80°$. After substituting the scattering amplitude s_a in (1.24) with s'_{vv} from (1.26), we obtain the expression for the matrix $\mathbf{S}$ in the general case of spheroid orientation determined by two angles, α and ψ.

$$\mathbf{S} = \begin{bmatrix} (s_a - s_b)\sin^2\psi \sin^2\alpha + s_b & (s_a - s_b)\sin^2\psi \sin\alpha\cos\alpha \\ (s_a - s_b)\sin^2\psi \sin\alpha\cos\alpha & (s_a - s_b)\sin^2\psi \cos^2\alpha + s_b \end{bmatrix}. \tag{1.27}$$

This relatively simple expression for the scattering matrix $\mathbf{S}$ is sufficient for interpretation of polarimetric properties of most hydrometeors at the 10, 5, and 3 cm wavelengths (designated with letters *S*, *C*, and *X*). It has been used extensively for modeling backscatter (e.g., Holt 1984; Ryzhkov 2001) and is similarly applied throughout this book. For more rigorous modeling of scattering wherein the backscatter rule does not hold, the reader is referred to Vivekanandan et al. (1991).

The elements of the backscatter matrix $\mathbf{S}$ are directly related to backscatter cross sections commonly used to quantify reflections from objects. The backscatter cross section of a scatterer is the area which if multiplied with the incoming power density would produce the same backscatter power density as an isotropic scatterer. To include polarization into this definition, let's assume the incident wave has polarization indexed by n (stands for either h or v) and consider the backscattered field E_n^b. According to (1.12), (1.13), and (1.14), the power density at the distance r from the scatterer in the backscatter direction ($\mathbf{k}_s = -\mathbf{k}_i$) is

$$\overline{|\vec{\mathbf{S}}|}_{mn} = \frac{|E_n^i|^2 |s_{mn}|^2}{2r^2\eta_o} \left(\mathrm{W\,m^{-2}}\right). \tag{1.28}$$

If $m = n$, the indicated power density ($\overline{|\vec{\mathbf{S}}|}_{hh}$ or $\overline{|\vec{\mathbf{S}}|}_{vv}$) is of the copolar component; otherwise ($\overline{|\vec{\mathbf{S}}|}_{hv}$ or $\overline{|\vec{\mathbf{S}}|}_{vh}$) it is of the cross-polar component. The cross-section definition σ_{mn} applicable to dual-polarization radars is the area that intercepts the incoming power density of the field E_n^i so that the backscattered power density at the antenna location corresponding to polarization m would be the same if the scatterers were radiating equally in all directions. This means

$$\overline{|\vec{\mathbf{S}}|}_{mn} = \frac{|E_n^i|^2 \sigma_{mn}}{8\pi r^2 \eta_o}. \tag{1.29}$$

Equating the power densities (1.28) and (1.29) yields

$$\sigma_{\mathrm{mn}} = 4\pi |s_{\mathrm{mn}}|^2 \left(\mathrm{m}^2\right). \tag{1.30}$$

1.3 Propagation Effects

Electromagnetic wave propagating through the atmosphere filled with hydrometeors acquires additional phase shift compared to what it would have in vacuum. Moreover, its amplitude decreases due to the presence of various gas molecules and hydrometeors. Each of the scatterers extracts a puny amount of energy from the wave and reradiates part of it in all directions while absorbing the rest. At microwave frequencies, the absorbed part is dominant (Bohren and Huffman 1983) except for very large hail and attenuation is quantified with the imaginary part of the effective refractive index $n_{h,v}$. In interaction with propagating EM fields, scatterers retard the wave and reduce its propagation speed. This increases the phase shift in proportion to the real part of $n_{h,v}$. In the absence of hydrometeors, the atmosphere is isotropic with respect to polarization (i.e., $n_h = n_v$), therefore, phase shifts and attenuation of the propagating wave are independent of polarization. This is not so if the atmosphere is filled with nonspherical oriented scatterers like raindrops or snowflakes because then $n_h \neq n_v$.

Each scatterer contributes its share to the effective refractive indexes $n_{h,v}$ (1.4) according to its forward-scattering amplitude. The contributions are linear and additive and n_h and n_v depend on the hydrometeor type, concentration, shape, orientation, and wavelength λ. These parameters can often be described with the distribution function $N(\boldsymbol{X})$ of the scatterer physical properties (size, shape, orientation, dielectric constant, etc.) characterized by vector $\boldsymbol{X}$. The function $N(\boldsymbol{X})$ is defined to produce the concentration of particles within the unit volume N_T (in m^{-3}):

$$N_T = \int N(\boldsymbol{X}) d\boldsymbol{X} \left(\mathrm{m}^{-3}\right). \tag{1.31}$$

The particles contribute to the average forward-scattering amplitude $< s^{(0)}_{\mathrm{hh,vv}} >$ per unit volume

$$< s^{(0)}_{\mathrm{hh,vv}} >= \int N(\boldsymbol{X}) s^{(0)}_{\mathrm{hh,vv}}(\boldsymbol{X}) d\boldsymbol{X} \left(\mathrm{m\,m}^{-3}\right), \tag{1.32}$$

where the angular brackets indicate probabilistic (ensemble) average of the particles' forward-scattering coefficients at horizontal and vertical polarizations.

Complex amplitudes (phasors) of the horizontally and vertically polarized waves defined in (1.11) are special solutions of the following two coupled differential equations (Oguchi 1983; Bringi and Chandrasekar 2001; Zhang 2016):